MSL CHEMCAM OBSERVATIONS OF CLORIDE SALTS IN GALE CRATER, MARS. N. H. Thomas[1] (nhthomas@caltech.edu), B. L. Ehlmann[1,2], P.-Y. Meslin[3], A. Cousin[3], O. Forni[3], W. Rapin[1], D. E. Anderson[1], S. Schröder[4,3], N. Mangold[5], R. C. Wiens[6], and O. Gasnault[3], [1]Geologic and Planetary Sciences, California Institute of Technology, Pasadena, CA, [2]Jet Propulsion Laboratory, Pasadena, CA, [3]Institut de Recherche en Astrophysique et Planétologie, Toulouse, France, [4]DLR, Berlin, Germany, [5]Laboratoire de Planétologie et Géophysique de Nantes, Université de Nantes, Nantes, France, [6]Los Alamos National Laboratory, Los Alamos, NM.

Introduction: Salts like chlorides, carbonates, and sulfates are evidence of the aqueous chemistry of past waters and can provide indications of past environmental conditions. Chloride deposits have been detected and mapped in hundreds of irregular depressions in the ancient Noachian and Hesperian aged terrains of the southern highlands of Mars [1]. The Mars Science Laboratory (MSL) Curiosity rover is currently investigating the sedimentary stratigraphy of Mt. Sharp, the mound at the center of Gale crater. The sediments in Gale, a 155-km wide impact crater that formed ~3.8-3.6 Ga ago, have been interpreted as fluvial deltaic and sandstone deposits [2] and stratified lake deposits [3]. Borate and chloride salts [4-6] along with possible desiccation features [7] have been reported in Gale suggesting potential evidence of a past drying lake.

Here we map detections of Cl using the Curiosity ChemCam instrument [8, 9] with the goal of identifying the type of chloride salt present and determining its formation mechanism.

Data and Methods: The ChemCam instrument onboard Curiosity uses Laser-Induced Breakdown Spectroscopy (LIBS) to provide fine-scale (350-550µm diameter) chemical analysis of targets up to 7 m away from the rover and also obtains high-resolution images using the Remote Micro-Imager (RMI). ChemCam is sensitive to the major elements as well as trace and volatile elements. Major element compositions are calculated for all targets [10, 11] but the detection and quantification of Cl using LIBS is complicated by relatively weak lines, interference with emission lines from other elements, and physical and chemical matrix effects. ChemCam has the advantage of a large dataset (>16,000 locations on the surface) with small spatial resolution.

We applied standard ChemCam data pre-processing [12] and remove the first five shots (contaminated by dust and subject to surface effects) before analysis. The Cl emission line at 837.8 nm increases monotonically with Cl content as shown by *Anderson et al.* [13]. We examined all spectra of ChemCam targets measured up to Sol 1815 of the mission to identify targets containing Cl. To count as a Cl detection, targets must have a clearly visible Cl peak at 837.8 nm and the peak must stand above the local continuum level and noise. To quantify Cl, we fit the local region (830-841 nm) with a pseudo-Voigt function and a local linear continuum using a Levenberg-Marquardt least squares minimization algorithm and report the fit Cl peak area. We normalize the peak area using the total intensity of the VNIR detector (Norm 3).

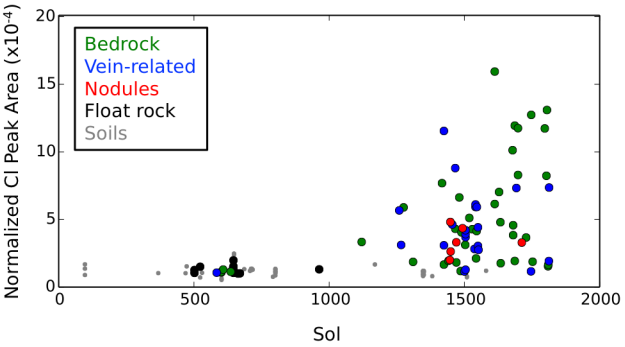

Figure 1: Normalized Cl peak area versus sol number for all targets where Cl is detected.

Results: Up to sol 1815, we have detected Cl in over 95 ChemCam targets (or ~140 observation points of >16,000 total). The majority of the rock-related detections occur after sol 1000 while most are in soil before this (Fig. 1). This corresponds approximately to the rover's transition from the Bradbury group into the Mt. Sharp group. All but 5 observation points of the bedrock-related detections occur in the Murray formation,

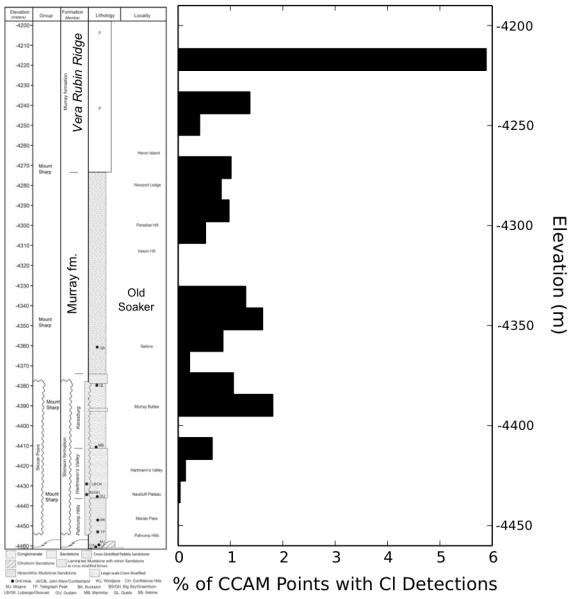

Figure 2: Gale stratigraphic column (left) [14] with % of CCAM points (Murray bedrock, vein-related, or nodules) where Cl is detected.

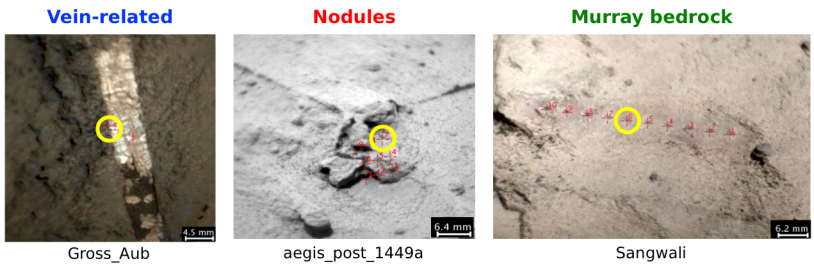

Figure 3: Examples of the target types described. Yellow circle indicates where Cl is detected.

the fine-grained, thinly-laminated mudstone facies which is the lowermost strata of the Mt. Sharp group. At the same time, an increase in the average normalized Cl peak area shows that the amount of Cl present in the target points increases.

The percent of ChemCam target points where Cl is detected stays relatively constant at < 2% throughout the Murray fm. but increases in recent sols in the upper Murray (Fig. 2). Above elevation -4230 m, the percent of points with Cl increases to almost 6%.

By visually inspecting Mastcam and RMI images for all Cl detection targets, we have sorted the non-float rock and soil points into three categories based on morphology (Fig. 3): bedrock (34 points), vein-related (24), and nodules (6). Most frequently, Cl is observed in isolated points of typical Murray bedrock material. In the case of the vein-related detections, Cl is generally found at the edge or border of the Ca-sulfate vein and the nearby bedrock although Cl has also been detected in vein centers and in dark vein targets [15]. ChemCam composition for these points shows mixing between Ca-sulfate and high Na_2O. We have also detected Cl in bedrock with nodular, resistant textures.

Cl content, quantified using the normalized Cl peak area, is positively correlated with weight percent Na_2O (Fig. 4). If the trend is 1:1 after conversion to molar abundance, we are likely observing halite (NaCl) or possibly Na-perchlorate ($NaClO_4$) or Na-chlorate ($NaClO_3$). We do not see a correlation between O and Cl suggestive of perchlorate/chlorate. Halite is also the most likely phase because CheMin has detected 1.1 +/- 0.3 (wt% crystalline) and 0.3 +/-0.1 (wt% bulk) halite in Quela where we observe Cl in the drill tailings [16]. For the Cl detection points, we also see a negative correlation between wt. % Na_2O and CaO possibly due to mixing with Ca-sulfates at vein edges. Applying the results of *Anderson et al.* [13], we find the highest observed mol fraction Cl (to total composition) is 0.3. We are currently using principal component analysis (PCA) to investigate if there are correlations with other elements.

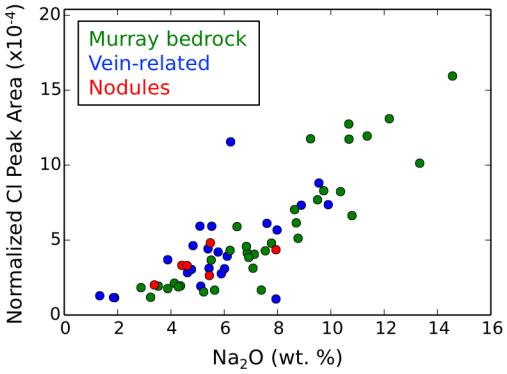

Figure 4: Positive correlation between wt. % Na_2O and Cl content suggestive of halite composition.

Discussion: Overall, the number of halite detections in Gale Crater is small although our detection limit is 3-6 wt. % Cl [12] or 3.4 wt. % as estimated from the martian dataset. We mostly see Cl present as sub-millimeter volumes in the bedrock (as evidenced by shot-to-shot profiles) and at vein edges. The small number of isolated detections is consistent with reworking and remobilization by later groundwaters. One possible history for halite emplacement is: 1) deposition of the Murray fm. in the Gale lake; 2) evaporation of lakewater and deposition of evaporitic salt layers including chlorides and borates in a near-shore environment; 3) burial of the Murray fm.; 4) episodic groundwater activity to dissolve, mobilize, and re-deposit the evaporites along veins and in complex nodular textures; 5) erosion to the present surface. The bedrock chlorides could also have been emplaced during early (initial phases of burial) or later (related to the nodules, concretions, etc.) diagenetic processes. Our continuing work is investigating the Cl and sulfate relationships and the implications of these salts for past water chemistry and environment.

Acknowledgements: This work was supported by a NSF Graduate Research Fellowship grant no. DGE-1144469 to N.H.T. and a MSL Participating Scientist grant to B.L.E.

References: [1] Osterloo M. M. et al. (2010) *JGR, 115*, E10012. [2] Grotzinger J. P. et al. (2015) *Science, 350(6257)*, aac7575. [3] Hurowitz J. A. et al. (2017) *Science, 356(6341)*, aah6849. [4] Gasda P. J. et al. (2017) *GRL, 44*, 8739. [5] Thomas N. H. et al. (2017) *LPS XLVIII*, Abstract #2756. [6] Forni O. et al. (2017) *LPS XLVIII*, Abstract #1838. [7] Stein N. T. et al. (2017) *LPS XLVIII*, Abstract #2387. [8] Wiens, R.C. et al. (2012) *Space Sci. Rev.*, 170, 167-227. [9] Maurice, S. et al. (2012) *Space Sci. Rev.*, 170, 95-166. [10] Clegg S. M. et al. (2017) *Spectrochimica Acta Part B, 129*, 64-85. [11] Anderson R. B. et al. (2017) *Spectrochimica Acta Part B, 129*, 49-57. [12] Wiens, R.C. et al. (2013) *Spectrochimica Acta Part B*, 82, 1-27. [13] Anderson D. E. et al. (2017) *JGR-Planets, 122*, 744-770. [14] Fedo C. et al. (2017) *LPS XLVIII*, Abstract #1689. [15] L'Haridon J. (2017) *LPS XLVIII*, Abstract #1328. [16] Achilles C. et al. (2018) in prep.